RSC Advances

Cite this: DOI: 10.1039/c0xx00000x
www.rsc.org/xxxxxx

COMMUNICATION

A General Approach towards the Efficient Catalysis in Pickering Emulsions Stabilized by Amphiphilic RGO-Silica Hybrid Materials

Xu-Rui Wei [a,b], Jun Liu [a,b], Yong Yang [a,b] and Li Deng*[a]

Received (in XXX, XXX) Xth XXXXXXXXX 20XX, Accepted Xth XXXXXXXXX 20XX
DOI: 10.1039/b000000x

A general approach towards efficient emulsion catalysis has been achieved using the amphiphilic RGO-silica hybrid materials with proper surface wettability and mesoporous structures. On the basis of the promising hybrids, Pickering emulsion with droplets from 20-100 µm was formed and a broad range of reactions was facilitated.

Emulsion catalysis is an environmentally benign approach to the reactions involving immiscible substrates or solvents, which are especially attractive for water mediated organic synthesis since most organic substrates are poorly soluble in water. As conventional methods, surfactants have been widely employed to emulsify the immiscible phases of an emulsion reaction system.[1] However, the major drawback of using surfactant molecules lies in the difficult recovery of them from the reaction mixture. To this end, recyclable surfactants have been developed based on polymeric materials and the Pickering emulsions stabilized by amphiphilic solid particles have also drawn great attention.[2] Moreover, Pickering emulsions were successfully applied in emulsion catalysis in recent years.[3-5] Favored by the irreversible adsorption of solid particles at the oil-water interface, Pickering emulsions are thermodynamically stable and provide a large reaction zone for immiscible substrates. After reactions the solid particles could be isolated by conventional filtration, recently developed pH-induced phase inversion[2d,4,5] and CO_2-triggered migration[2e]. As an excellent example, Resasco *et al*. fabricated the amphiphilic hybrid nanoparticles of carbon nanotubes (CNTs) and inorganic oxides via the chemical vapor deposition on silica and magnesia supported transition metal catalysts.[3b] Owing to the integration of the intrinsic oleophilicity of CNTs and the hydrophilicity of inorganic oxides, the catalysts could stabilize the biphasic reaction system and control the hydrodeoxygenation of bio-derived oxygenates in aqueous phase or both phases by selective locating the active sites (Pd nanoparticles) on the surface of the amphiphilic hybrids. Another route for amphiphilic solid particles synthesis is the post graft using hydrophobic silanes. For instance, the octadecyltrichlorosilane decorated HY zeolites have been prepared for alkylation of *m*-cresol and 2-propanol in a biphasic system.[3d] Yang *et al*. reported the octyl-triamine bifunctionalized silica microspheres could support palladium for the hydrogenation of styrene in emulsion and the as-prepared catalysts could be readily recycled by the pH-triggered phase transfer.[4] Using carbonaceous materials whose surfaces contain oxygenated functional groups, Zhou *et al.* presented the reduction of *p*-nitroanisole in the pH-dependent irreversible Pickering emulsions.[5]

In this contribution, we attempt to pave a new way to synthesize amphiphilic solid catalysts via the combination of oleophilic graphene material and hydrophilic silica. Graphene, a monolayer of sp^2-hydrid carbon atoms, has received increasing interest from the research fields of electrodes, supercapacitors, photoelectrics and catalysis as well.[6] However, the graphene materials have not gained sufficient attention in emulsion catalysis, though graphene oxide (GO) has been recognized as good surfactant to stabilize Pickering emulsions.[7] We envision that the rational design of amphiphilic catalysts with tuneable surface wettability could be realized through the combination of desired amount of graphene and silica. To prepare the hybrids, we choose GO and tetraethoxysilane as starting materials to build the oleophilic moiety reduced graphene oxide (RGO) and hydrophilic moiety mesoporous silica (SBA-15) (Scheme 1). The advantages of this approach lie in the following aspects: 1) GO, a relatively stable solid, is convenient to use and to control the content in the final hybrids, making the synthetic method reproducible; 2) Owing to the numerous oxygenate functionalities, GO can be well dispersed together with silane and template in water, facilitating the integration of the two moieties; 3) GO obtained from the abundant graphite via scalable methods could make the synthesis of the amphiphilic materials economically feasible; 4) The porous structures contributed by the hydrophilic moiety enable them to accommodate both active sites and substrates. With the RGO-silica based amphiphilic materials, we demonstrate that they could stabilize Pickering emulsions and efficiently catalyze a broad range of reactions, including oxidation, reduction, hydrogenation, hydrolysis and chloromethylation.

The GO with thickness of *ca.* 1 nm (Figure S1) was prepared according to the modified Hummer's method.[8] Desired amount of the GO was homogeneously dispersed in water and then mixed with the template P123 and HCl. After 2h stirring, tetraethoxysilane was added to the mixture. The following synthetic steps followed the conventional method for the SBA-15 preparation,[9] except for the addition of excess amount of hydrazine during the hydrothermal treatment. After hydrothermal treatment, the observation of black hydrogel suggested the formation of 3D network structure in the presence of GO and silane. After template removal at 600 °C in Ar, the resulting amphiphilic hybrids with colours from light gray to black were

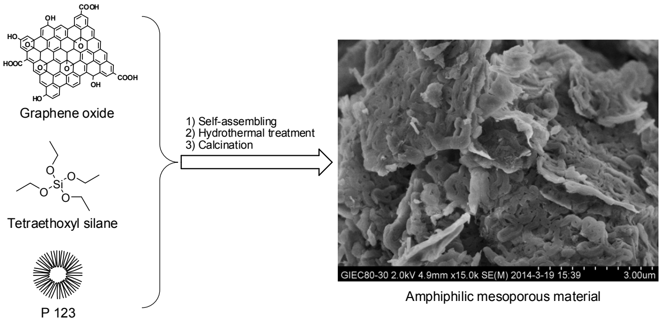

Scheme 1 Schematic diagram of the synthesis of the amphiphilic material with mesopores

denoted as SBA-G-x, where x referred to the weight percent of the RGO (based on the GO loading and elemental analysis of GO). Considering the surface activity of GO, we wondered whether the addition of GO would influence the P123 micelle formation and the mesoporous structure of the final products. According to the N_2 isothermal adsorption-desorption analysis (Figure 1a and S3), the hybrid materials present typical IV hysteresis curves, indicative of the mesoporous structure. The BET surface areas range from 567 m^2 to 623 m^2. The BJH pore volume and BJH average pore size are 1.14~1.16 cm^3g^{-1} and 6.6~7.7 nm (Table S1). These properties are similar to those of pure SBA-15 and suggest that the hybrids could act as ideal supports or catalysts due to the high surface area and mesopores. The X-ray diffraction (XRD) of SBA-G-5 exhibits a strong (100) diffraction peak at 0.90 ° and two weak diffraction peaks corresponding to the (110) and (200) directions, revealing the periodical mesoporous structure, which is consistent with the results of N_2 isothermal adsorption-desorption analysis.

In order to study the microstructure of the hybrid materials, scanning electron microscopy (SEM) and transmission electron microscopy (TEM) have been employed to investigate the hybrid materials. The SEM image (Figure 2a) shows that the SBA-G-5 consists of rod-like granules with the diameter less than1 µm, which are aggregated into bulk phase. Besides the rod-like granules, we also observed some curling layers distributed randomly in the bulk phase. High resolution images (Figure 2b and 2c) reveal that the layers are similar to these of GO (Figure S2d) but bear worm-like structures. These might be generated from the deposition of the periodic ordered mesoporous silica onto the large surface of GO during the hydrothermal process.[6h] The electron dispersive spectrometer (EDS) reveals the RGO are distributed in silica matrix homogeneously at µm scale (Figure S4). After gridding and sonicating in water, the aggregated granules could be well dispersed (Figure 2d). Moreover, the TEM images present the ordered mesoporous channels and hexagonal honeycomb-like cross sections, which are typical morphology of conventional SBA-15 materials. These results suggest that the formation of the ordered mesoporous structure will not be significantly influenced by the addition of GO.

Raman spectroscopy was usually employed to evaluate the state of carbon materials. In this study, the RGO in hybrid material was also examined by this technique. As shown in Figure S5a, the ratio of the D band (1344 cm^{-1}) and G band (1598 cm^{-1}) intensity is *ca.* 0.68, which is much lower than that of GO (0.97, Figure S2a). This suggests that the oxygenates in GO were reduced by hydrazine. Moreover, the X-ray photoelectron

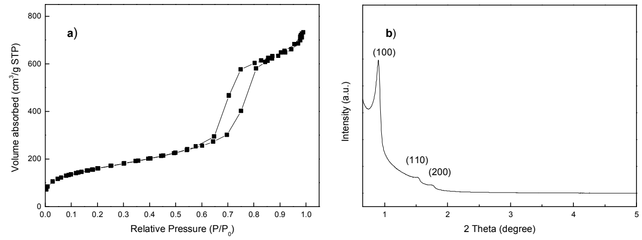

Fig. 1 a) N_2 isothermal adsorption-desorption isotherm of SBA-G-5; b) XRD profile of SBA-G-5

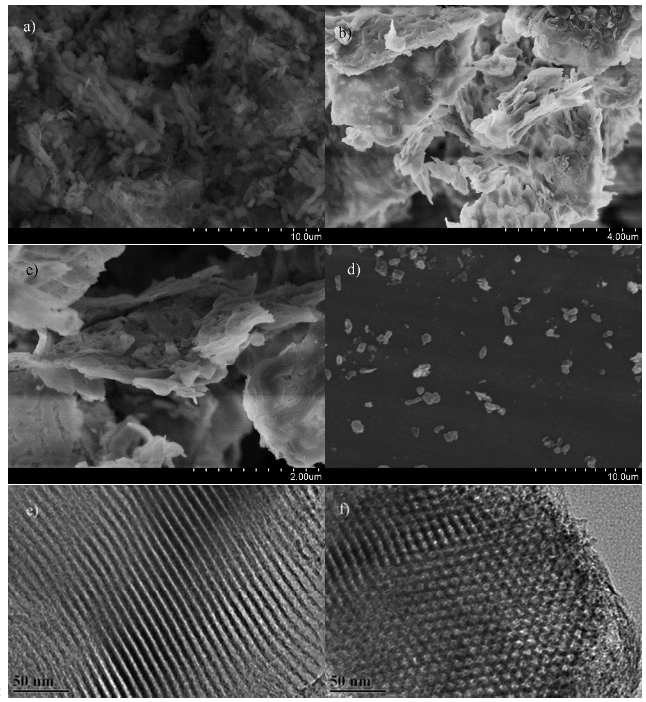

Fig. 2 Electron microscopy analysis of SBA-G-5.a)~d) SEM images; e) and f) TEM images

spectroscopy (XPS, Figure S5b) of SBA-G-5 shows a strong C_{1s} peak at the binding energy of 284.4 eV, associated with the sp^2 C=C species. Compared to that of GO (Figure S2b), the intensities of C_{1s} peak at higher binding energy, corresponding to the hydroxyl, epoxyl, carbonyl and carboxyl, are much lower, which agree with the results of Raman spectroscopy.

To verify the amphiphilicity of the hybrid materials, a comparison of the migration of pure SBA-15 and SBA-G-5 in water-decalin biphasic system was carried out. It is clear that the hybrid material SBA-G-5 migrated to the biphasic interface, whereas the SBA-15 remained in the bottom layer (Figure S6). Furthermore, the surface wettability is an essential property for the rational design and preparation of amphiphilic materials suitable for stabilizing Pickering emulsions. Owing to the porous structure, the materials quickly soaked water and decalin. Thus we measured the contact angles of water on the amphiphilic materials in decalin, instead of the air-water or air-decalin contact angles. The pellets of SBA-G-x were immersed in decalin in a quartz cell and water droplets were injected onto their surfaces. Figure 3a shows that the hydrophilic SBA-15 and SBA-G-1 have small contact angles of 56.8 ° and 57.5°, respectively. Note that the value dramatically increased to 82.1° when 5 wt% of RGO was mixed. For SBA-G-10, the value is 100.7 °. This could be

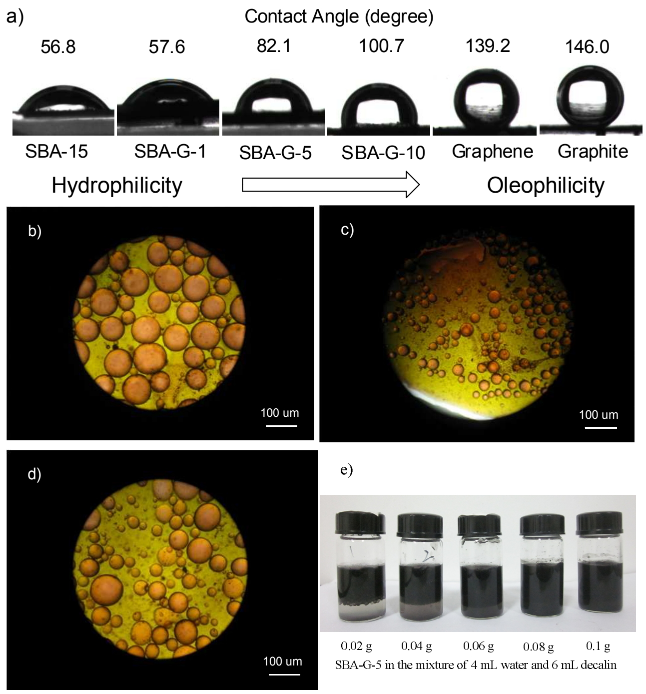

Fig. 3 a) Decalin-water contact angle measurements, optical microscopy of Pickering emulsion stabilized by 1 wt%, b) SBA-G-1, c) SBA-G-5 and d) SBA-G-10 and e) Photograph of the Pickering emulsions stabilized by SBA-G-5

attributed to the strong hydrophobicity of RGO, whose contact angle is 139.2 °, close to the value of pristine graphite (146.0 °). These values reveal that the SBA-G-5 and SBA-G-10 make good balance between the hydrophilic silica and oleophilic RGO and they may act as ideal "emulsifiers" to stabilize Pickering emulsions.

More importantly, the results also indicate that the present method is feasible and convenient to control the surface wettability of the amphiphilic.

Further characterization by FT-IR (Figure S7) demonstrates that the intensities of the stretching vibration of hydroxyl decrease with the raise in RGO amount, which could be attributed to the enhanced surface hydrophobicity of the hybrids caused by the higher loading of RGO.

In Figure 3c, optical microscopy images of emulsions stabilized by SBA-G-5 exhibit that oil-in-water (O/W) emulsions are stabilized by the hybrid granules and the size of emulsion droplets ranges from 20 μm to 100 μm. By contrast, more hydrophilic SBA-G-1 and hydrophobic SBA-G-10 afford larger O/W emulsion droplets (Figure 3b and 3d). Figure 3e shows that the emulsion volume of the mixture of 4 mL water and 6 mL decalin goes up until 0.08 g SBA-G-5 is added, resulting in the disappearance of the interface. Besides, the ratio of oil to water also influences the emulsion volume. When the ratio changed from 6:4 to 8:2, the emulsion shifted from O/W to W/O type and SBA-G-5 migrated into the bottom layer (Figure S8). Note that the as-prepared Pickering emulsions are thermodynamically stable as we observed no sedimentation or coalescence after 1-month stand.

With the amphiphilic hybrid materials in hand, we performed five reactions (chloromethylation, hydrolysis of benzyl chloride, reduction of nitrobenze, hydrogenation of vanillin and oxidative desulfurization) to testify their versatility and efficiency for emulsion reactions. We began the catalytic tests with the chloromehtylation of toluene and hydrolysis of benzyl chloride. These organic substrates are insoluble in aqueous medium, so the reactions usually carried out in the presence of phase transfer catalysts.[10] As shown in table S2, the amphiphilic SBA-G-5 enables the toluene to react with formaldehyde and hydrogen chloride in aqueous phase, giving chloromethyl toluene with a yield of 98 %. By contrast, the yield is 72 % in the presence of the pure SBA-15. The reaction with surfactants PEG-1000 and octadecyltrimethyl ammonium chloride (OTAC) could deliver yields of 85 % and 81 %, respectively. Similarly, the results of the hydrolysis of benzyl chloride (Table S3) also demonstrate that SBA-G-5 is an efficient phase transfer catalyst for emulsion reaction of immiscible substrates.

The reduction of nitroaromatics to anilines is an important industrial process. However, the commonly used reducing agents, such as Na_2S, $NaBH_4$ and hydrazine are aqueous soluble while nitroaromatics are poorly soluble in water.[5,11] To this end, we performed the reduction of nitroaromatics in Pickering emulsions stabilized by the hybrid materials. Table 1 shows that only 9 % nitrobenzene is reduced to aniline by Na_2S without phase transfer catalyst. For the surfactants PEG-1000 and OTAC, the yield of aniline increases to 20 %. It has been reported that graphene is an effective catalyst for the reduction of nitroaromatics.[6g] When 5 mg RGO is added to this reaction, the yield is also improved to 29 %. To our delight, the amphiphilic SBA-G-5 enables the reaction with a high yield of 78 % (Table 1, entry 5). By contrast, the physical mixture of RGO and SBA-15 could not deliver the yield as high as the amphiphilic SBA-G-5 does (Entry 6). Based on these results, we believe that the good performance of SBA-G-5 should be attributed to the synergic effect of the amphiphilic surface that enhances the mass transfer between the two immiscible phases and the RGO moiety that provides the catalytic sites.

Optimized results could be achieved through varying the volume ratio of water to decalin (Entry 7~9). 85 % of aniline could be obtained at the water : decalin ratio of 4:6. Furthermore, when using SBA-G-10 as catalyst, a full conversion of nitrobenzene into aniline has been achieved. Using other analogues of nitrobenzene as substrates (i.e. *p*-methylnitrobenzene, *p*-methoxylnitrobenzene, *m*-dinitrobenzene and *p*-chloronitrobenzene, entry 12~15), the yields of anilines range from 73 % to 99 %.

Table 1. Reduction of nitroaromatics in water-decalin mixtures

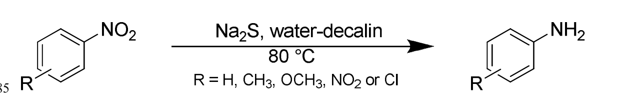

Entry[a]	Catalysts	Catalyst loading (mg)	$V_{water}/V_{decalin}$	Yield (mol%)
1	--	0	7:3	9
2	PEG-1000	100	7:3	20
3	OTAC	100	7:3	20
4	RGO	5	7:3	29
5	SBA-G-5	100	7:3	78

6	RGO + SBA-15	100	7:3	34
7	SBA-G-5	100	6:4	80
8	SBA-G-5	100	4:6	85
9	SBA-G-5	100	3:7	82
10	SBA-G-10	80	7:3	100
11	SBA-G-15	80	7:3	98
12[b]	SBA-G-5	100	7:3	99
13[b]	SBA-G-5	100	7:3	97
14[b]	SBA-G-5	100	7:3	90[c]
15[b]	SBA-G-5	100	7:3	73

[a] Reaction conditions: for entry 1~11, nitrobenzene (0.31 g, 2.5 mmol) and Na_2S (0.58 g, 7.4 mmol) in a water-decalin biphasic system with a total volume of 20 mL reacted at 80 ºC for 6 h. [b] entry 12-15, *p*-methylnitrobenzene (0.25 mmol), *p*-methoxylnitrobenzene (2.5 mmol), *m*-dinitrobenzene (2.5 mmol) and *p*-chloronitrobenzene (2.5 mmol) were reduced at 80 ºC for 8 h, respectively. [c] yield of *m*-diaminobenzene.

In addition to the role of phase transfer catalysts, we believe that the hybrid materials could act as supports to anchor metal nanoparticles and other active phases on their large inner surfaces. In this aspect, Pd@SBA-G-5 has been prepared for the selective hydrogenation of vanillin, which is an important model compound of fast pyrolysis oil and prone to distribute in aqueous media. In principle, Pd nanoparticles lean to deposit on the hydrophilic silica side, because the surface area is mainly contributed by the silica matrix and its hydroxyl abundant surface are more readily to anchor Pd nanoparticles than that of RGO. Thus the hydrogenation of vanillin is considered to take place mainly in aqueous phase. On the other hand, hydrogen gas has higher solubility in organic solvents than in water, thus the water-decalin emulsion stabilized by the amphiphilic hybrids could also facilitate the mass transfer of hydrogen gas for the hydrogenation.[3b] Table 2 shows the results of the hydrogenation of vanillin in water-decalin emulsion stabilized by Pd@SBA-G-5. According to the products distribution, the amphiphilic catalyst renders the hydrogenation of vanillin to vanillin alcohol (VA) at the first hour at 90 ºC while 2-methoxy-4-methyl phenol (MMP) is generated as minor product. However, after 4-hour reaction, most VA is converted into MMP though hydrodeoxygenation. By comparison, both SBA-15 and SBA-G-5 showed no catalytic activity for hydrogenation due to the absence of palladium (Entry 3 and 4). At higher temperature (150 ºC), Pd@SBA-G-5 allows the hydrogenation of vanillin towards MMP with high conversion and selectivity as well. Moreover, in all cases, even at 200 ºC for 4 hours, no decarbonylation product 2-methoxylphenol has been observed. These results suggest that the hydrogenation of vanillin could occur selectively in aqueous phase in the presence of Pd@SBA-G-5.

Table 2. Pd@SBA-G-5 catalyzed hydrogenation of vanillin in water-decalin biphasic systems.

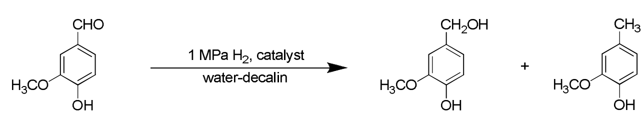

Entry[a]	Temperature (ºC)	Reaction time (h)	Conversion of vanillin (mol%)	Selectivity (%)	
				VA	MMP
1	90	1	78	83	17
2	90	4	86	0	100
3[b]	90	4	0	-	-
4[c]	90	4	0	-	-
5	150	1	90	0	100
6	150	4	98	0	100
7	200	4	100	0	100

[a] Reaction condition: vanillin (0.21 g), water (15 mL), decalin (15 mL) and Pd@SBA-G-5 (5 wt% Pd, 0.1 g) were added to a 50 mL autoclave, vigorously stirred and reacted under 1 MPa H_2. [b] Pure SBA-15 was used as catalyst. [c] SBA-G-5 was used as catalyst.

Finally, the model reaction of oxidative desulfurization has been investigated with the amphiphilic hybrids supported heteropoly acids (HPAs) catalyst. It was reported that the integrated catalysts containing heteropoly anions and amine cations could deeply remove dibenzothiophene (DBT), a model compound of sulfur impurity in diesel, through the catalytic oxidation with H_2O_2.[12] Thus, we attempt to perform the reaction using RGO-silica hybrids supported HPAs as both emulsifiers and catalysts. In Table 3, it is clear that the autocatalytic oxidation is not sufficient to remove DBT (Entry 1 and 2). The amphiphilic hybrid SBA-G-5 could convert 33 % DBT due to the emulsion effect. It is noteworthy that the $H_3PMo_{12}O_{40}$@SBA-G-5 gives much better performance than that using $H_3PMo_{12}O_{40}$ or $H_3PW_{12}O_{40}$ solely (Entry 4-6). In the presence of $H_3PMo_{12}O_{40}$@SBA-G-5, the sulfur content could be reduced to less than 10 ppm. For $H_3PW_{12}O_{40}$@SBA-G-5, the conversion of DBT can also reach 92 %. Regarding the leaching of HPAs from the catalysts in water, we deposit the Cs substituted HPAs onto the surface of SBA-G-5 for this reaction. Consequently, the conversion of DBT is 99 % and 94 % in the presence of $Cs_{2.5}H_{0.5}PMo_{12}O_{40}$@SBA-G-5 and $Cs_{2.5}H_{0.5}PW_{12}O_{40}$@SBA-G-5, respectively. For $Cs_{2.5}H_{0.5}PMo_{12}O_{40}$@SBA-G-5, no obvious deactivation occurred and 90 % dibenzothiophene could be converted at the fifth recycling run (Entry 8~12). The slight decrease in conversion is partially caused by the weight loss of catalyst during the filtration. By changing the ratio of water : decalin or replacing water with acetonitrile, the DBT could be near completely removed (Entry 14 and 15). The effect of reaction time, temperature and the structure of thiophene contaminants on this oxidative conversion have also been investigated (Figure S9).

Table 3. Oxidative desulfurization in biphasic model systems.

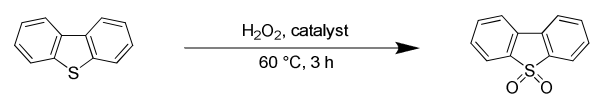

Entry[a]	Catalysts	Catalyst loading (mg)	Conversion of DBT (mol%)
1	--	0	3
2	PEG-1000	80	8
3	SBA-G-5	80	33
4	$H_3PW_{12}O_{40}$	20	27
5	$H_3PMo_{12}O_{40}$	20	35
6	$H_3PMo_{12}O_{40}$@SBA-G-5	80	99
7	$H_3PW_{12}O_{40}$@SBA-G-5	80	92
8	$Cs_{2.5}H_{0.5}PMo_{12}O_{40}$@SBA-G-5	80	99
9[b]	$Cs_{2.5}H_{0.5}PMo_{12}O_{40}$@SBA-G-5	80	98
10[b]	$Cs_{2.5}H_{0.5}PMo_{12}O_{40}$@SBA-G-5	80	96
11[b]	$Cs_{2.5}H_{0.5}PMo_{12}O_{40}$@SBA-G-5	80	93

12[b]	$Cs_{2.5}H_{0.5}PMo_{12}O_{40}$@SBA-G-5	80	90
13	$Cs_{2.5}H_{0.5}PW_{12}O_{40}$@SBA-G-5	80	94
14[c]	$Cs_{2.5}H_{0.5}PMo_{12}O_{40}$@SBA-G-5	80	99
15[d]	$Cs_{2.5}H_{0.5}PMo_{12}O_{40}$@SBA-G-5	80	99

[a] Reaction condition: dibenzothiophene (25 mg, 0.13 mmol) in decalin (7 mL) and H_2O_2 (0.5 M, 3 mL) reacted at 60 ºC for 3 h. [b] Entry9-12: dibenzothiophene conversion in the 2nd~5th runs. [c] 8 mL decalin and 2 mL water were used. [d] 5 mL decalin and 5 mL acetonitrile were used.

Conclusions

In summary, we have successfully prepared the RGO-silica based amphiphilic hybrid materials for efficient catalysis in Pickering emulsion. These materials could be adjusted to a proper wettability to act as solid emulsifier and also have large surface area to accommodate active sites and substrates to facilitate catalytic conversions. The excellent performance in five classes of reactions highlights the superiority and feasibility of these amphiphilic catalysts based on the RGO-silica hybrids.

Acknowledgements

The authors are grateful to Natural Science Foundation of China (21302230) and Youth Innovation Promotion Assosiation, CAS for the financial support.

Notes and references

[a] *Key Laboratory of Cellulose and Lignocellulosics Chemistry, Guangzhou Institute of Chemistry, Chinese Academy of Sciences, Guangzhou 510650 China.*
Fax: (+86)2085232917; E-mail: dengli@gic.ac.cn
[b] *University of Chinese Academy of Sciences, Beijing 100039, China.*

† Electronic Supplementary Information (ESI) available: [details of any supplementary information available should be included here]. See DOI: 10.1039/b000000x/

1 a) C. M. Starks, *J. Am. Chem. Soc.,* 1971, **93**, 195; b) A. W. Herriott, D. Picker, *J. Am. Chem. Soc.,* 1975, **97**, 2345; c) E. V. Dehmlow, *Angew. Chem. Int. Ed.,* 1977, **16**, 493; d) H. H. Freedman, *Pure Appl. Chem.,* 1986, **58**, 857.
2 a) D. E. Bergbreiter, *Top. Curr. Chem.* 2004, **242**,113; b) S. Handa, J. C. Fennewald, B. H. Lipshutz, *Angew. Chem. Int. Ed.,* 2014, **53**, 3432; c) S. U. Pickering, *Journal of the Chemical Society, Transactions,* 1907, **91**, 2001; d) J. Giermanska-Kahn, V. Schmitt, B. P. Binks, F. Leal-Calderon, *Langmuir,* 2002, **18**, 2515; e) B. P. Binks, C. P. Whitby, *Colloid Surface A,* 2005, **253**, 105; f) B. P. Binks, J. A. Rodrigues, *Angew. Chem. Int. Ed.,* 2005, **44**, 441; g) J. H. Jiang, Y. Zhu, Z. G. Cui, B. P. Binks, *Angew. Chem. Int. Ed.,* 2013, **52**, 12373; h) Y. Zhu, L. H. Lu, J. Gao, Z. G. Cui, B. P. Binks, *Colloid Surface A*, 2013, **417**, 126; i) B. P. Binks, L. Isa, A. T. Tyowua, *Langmuir,* 2013, **29**, 4923.
3 a) M. Shen, D. E. Resasco, *Langmuir,* 2009, **25,** 10843; b) S. Crossley, J. Faria, M. Shen, D. E. Resasco, *Science,* 2010, **327**, 68; c) M. P. Ruiz, J. Faria, M. Shen, S. Drexler, T. Prasomsri, D. E. Resasco, *Chemsuschem,* 2011, **4**, 964; d) P. A. Zapata, J. Faria, M. P. Ruiz, R. E. Jentoft, D. E. Resasco, *J. Am. Chem. Soc.,* 2012, **134**, 8570; e) J. Faria, M. P. Ruiz, D. E. Resasco, *Adv. Synth. Catal.,* 2010, **352**, 2359.
4 H. Q. Yang, T. Zhou, W. J. Zhang, *Angew. Chem. Int. Ed.,* 2013, **52**, 7455.
5 a) H. Y. Tan, P. Zhang, L. Wang, D. Yang, K. B. Zhou, *Chem. Commun.,* 2011, **47**, 11903; b) D. Z. Ni, L. Wang, Y. H. Sun, Z. R. Guan, S. Yang, K. B. Zhou, *Angew. Chem. Int. Ed.*, 2010, **49**, 4223.
6 a) A. K. Geim, K. S. Novoselov, *Nat. Mater.,* 2007, **6**, 183; b) A. K. Geim, *Science,* 2009, **324**, 1530; c) D. Chen, H. B. Feng, J. H. Li, *Chem. Rev.,* 2012, **112**, 6027; d) W. J. Xiao, Z. Y. Sun, S. Chen, H. Y. Zhang, Y. F. Zhao, C. L. Huang, Z. M. Liu, *Rsc Adv.,* 2012, **2**, 8189; e) J. S. Cheng, G. C. Zhang, J. H. Du, L. Y. Tang, J. Y. Xu, J. H. Li, *J. Mater. Chem.,* 2011, **21**, 3485; f) A. B. Dongil, B. Bachiller-Baeza, A. Guerrero-Ruiz, I. Rodriguez-Ramos, *J. Catal.,* 2011, **282**, 299; g) Y. J. Gao, D. Ma, C. L. Wang, J. Guan, X. H. Bao, *Chem. Commun.,* 2011, **47**, 2432; h) L. Shang, T. Bian, B. H. Zhang, D. H. Zhang, L. Z. Wu, C. H. Tung, Y. D. Yin, T. R. Zhang, *Angew. Chem. Int. Ed.,* 2014, **53**, 250.
7 a) Y. Q. He, F. Wu, X. Y. Sun, R. Q. Li, Y. Q. Guo, C. B. Li, L. Zhang, F. B. Xing, W. Wang, J. P. Gao, *Acs Appl. Mater. Inter.,* 2013, **5**, 4843; b) M. Y. Tang, X. R. Wang, F. Wu, Y. Liu, S. Zhang, X. B. Pang, X. X. Li, H. X. Qiu, *Carbon,* 2014, **71**, 238.
8 a) W. S. Hummers, R. E. Offeman, *J. Am. Chem. Soc.,* 1958, **80**, 1339; b) Y. Zhu, D. K. James, J. M. Tour, *Adv. Mater.,* 2012, **24**, 4924.
9 D. Y. Zhao, J. L. Feng, Q. S. Huo, N. Melosh, G. H. Fredrickson, B. F. Chmelka, G. D. Stucky, *Science,* 1998, **279**, 548.
10 a) Q. F. Liu, W. Wei, M. Lu, F. Sun, J. Li, Y. C. Zhang, *Catal. Lett.,* 2009, **131**, 485; b) Y. L. Hu, Q. Ge, Y. He, M. Lu, *Chemcatchem,* 2010, **2**, 392.
11 G. D. Yadav, S. V. Lande, *Adv. Synth. Catal.,* 2005, **347**, 1235.
12 C. Li, Z. X. Jiang, J. B. Gao, Y. X. Yang, S. J. Wang, F. P. Tian, F. X.Sun, X. P. Sun, P. L. Ying, C. R. Han, *Chem-Eur J.,* 2004, **10**, 2277.